where $R$ $R_*$ refer to the original vortex and $R'$, $R_*'$ to the image vortex at the inverse point.

As a result, we conclude that

$$\frac{R}{R_*} = \frac{R'}{R_*'}$$

or

$$R_*' = \frac{R'}{R} R_* \tag{4}$$

However, the equation of the circle can be written in the form

$$\frac{R'}{R} = \frac{a - (a^2/c)}{c - a} = \frac{a}{c}$$

since in Cartesian coordinates this becomes

$$\frac{(x - a^2/c)^2 + y^2}{(x-c)^2 + y^2} = \frac{a^2}{c^2}$$

which gives on simplification

$$x^2 + y^2 = a^2$$

It follows from Eq. (4) that the core radius of the image vortex at the inverse point is $R_*'$, where

$$R_*' = \frac{a}{c} R_*$$

Since the core radius of the vortex at the origin does not affect the condition of tangential velocity at the circle and since we will not be interested in points inside the circle, it is proposed to use an inviscid vortex at the origin.

## V. Conclusions

This paper has described the techniques used in the SUBSIM mathematical model to represent the flow around a body of revolution at an angle of attack. These involve the representation of the measured vorticity contours by a series of discrete Rankine vortices. The condition for the vortices to merge has been examined. Expressions for the Rankine vortex image within the circular body have also been developed. These techniques have application in the treatment of vortical flows close to circular bodies: submarines, airships, missiles, and offshore structures.

## References

[1]Lloyd, A. R. J. M., "Progress Towards a Rational Method of Predicting Submarine Manoeuvres," Paper 21, *Royal Inst. of Naval Architects Symposium on Naval Submarines,* Vol. II, Royal Inst. of Naval Architects, London, May 1983, p. 12.

[2]Lloyd, A. R. J. M., "Developments in the Prediction of Submarine Manoeuvres," *Undersea Defense Technology Conference Proceedings,* Microwave Exhibitions and Publishers, London, 1988, pp. 134–138.

[3]Mendenhall, M. R., Perkins, S. C., and Lesieutre, D. J., "Prediction of the Aerodynamic Characteristics of Flight Vehicles in Large Unsteady Manoeuvres," *Proceedings of the 15th Congress of the International Council of the Aeronautical Sciences,* edited by P. Santini and R. Stautenbel, Vol. 2, AIAA, New York, 1986, pp. 662,675.

[4]Glauert, H., *The Elements of Aerofoil and Airscrew Theory,* Cambridge Univ. Press, London, 1947.

[5]Lloyd, A. R. J. M., and Campbell I. M. C., "Experiments to Investigate the Vortices Shed from a Body of Revolution," *Aerodynamic and Related Hydrodynamic Studies Using Water Facilities,* AGARD CP 413, 59th Meeting of the AGARD Fluid Dynamics Panel Symposium, Montery, CA, 1986, Paper 33, pp. 1–22.

[6]Lloyd, A. R. J. M., "Experiments to Investigate the Vorticity Shed by a Body of Revolution in Curved Flow," *Advances in Underwater Technology, Ocean Science and Offshore Engineering,* Vol. 15, Technology Common to Aero and Marine Engineering, Society for Underwater Technology, London, 1988, pp. 73–84.

[7]Freestone, M. M., "Vorticity Measurements by a Pressure Probe," *Aeronautical Journal,* Jan. 1988, p. 29–35.

# Numerical Simulation of Vortex Unsteadiness on a Slender Body at High Incidence

David Degani*
*NASA Ames Research Center, Moffett Field, California 94035*

## Introduction

RECENT studies (e.g., Refs. 1–3), conducted on two-dimensional and inclined cylinders of various cross-sectional shapes throughout the angle-of-attack range, have indicated that a high degree of flow unsteadiness may be present because of various phenomena. These include low-frequency three-dimensional effects, asymmetry-related vortex flipping, moderate-frequency von Kármán shedding, and higher frequency transition-related phenomena. In several cases, combinations of the phenomena have been found to coexist.

The study of Kourta et al.[1] presents information concerning small-scale, shear-layer vortices on two-dimensional cylinders for Reynolds numbers ranging from $Re_D = 2 \times 10^3$ to $6 \times 10^4$. Hot-wire power spectra measured at points in the shear layer showed two peaks, the first corresponding to the von Kármán vortex shedding and the second to a much higher frequency associated with motion on the shear layer. Investigations of Wei and Smith[2] on two-dimensional circular cylinders provided additional evidence of the transition waves and showed that these waves are highly three dimensional.

Poll[3] investigated the flow over a long cylinder (noncircular cross section) at Reynolds numbers ranging from $4.5 \times 10^5$ to $8.3 \times 10^5$ and angles of incidence ranging from 55 to 70 deg. He found that the boundary layer is susceptible to time-dependent disturbances that grow to large amplitude before the onset of transition. At the lower end of the Reynolds number range studied (prior to the transition to turbulence), a high-frequency rider was measured superimposed on a low-frequency von Kármán-like wave.

Preliminary computations[4] of laminar flow around an ogive-cylinder body at large incidence indicated that the computed wake was asymmetric and also unsteady. Close examination of the solution showed that shear-layer vortices were being shed into the leeside vortex flowfield at a high frequency. Following the numerical finding, Degani and Zilliac[5] conducted an experiment that demonstrated that the flowfield around an ogive-cylinder body at angles of attack above 30 deg was also highly unsteady. Three distinct unsteady flow phenomena were identified. These phenomena included a low-frequency von Kármán vortex shedding, a high-frequency shear-layer unsteadiness, and a vortex interaction at moderate frequency. The shear-layer fluctuations were found to decrease in amplitude and become intermittent as the angle of attack approach-

Received Oct. 15, 1990; revision received March 1, 1991; accepted for publication March 6, 1991. 

*Associate Professor, Faculty of Mechanical Engineering, on leave from Technion—Israel Institute of Technology, Haifa, Israel. Associate Fellow AIAA.

ed 90 deg. Figures 1 show a sequence of successive frames taken with a high-speed movie camera (unpublished data—Degani and Zilliac, 1988) at angle of attack of 40 deg and $Re_D = 2.6 \times 10^4$. The black areas in the photographs show a cross section of smoke that was entrained into the vortices near the tip. Waves can be seen to move at high speed along the shear layer (and are indicated on the photographs by the arrows). These waves were found to be associated with the high-frequency surface pressure fluctuations that were measured at the same axial location. Figures 2 (taken from Ref. 5) show power spectra of the surface pressure measurement at angles of attack between 30 and 85 deg. Figure 2a presents the low-frequency range and shows that a peak is formed at a Strouhal number (dimensionless frequency, $S = fD/U_\infty$) of about $S = 0.2$ as the angle of attack is increased. This peak was associated with the von Kármán vortex shedding from the aft part of the body. Figure 2b presents the high-frequency range and shows peaks near $S = 6$ for angles of attack between 30 and 60 deg. These peaks were associated with the motion of the high-speed shear-layer vortices. The vortex interaction was limited to areas where pairs of counter-rotating vortices curve away from the surface of the body.

In the current work, a thin-layer Navier-Stokes solver[6] was used to compute unsteady flows around an ogive-cylinder body at high incidence, and the results were compared with available experimental data. The aim was to determine whether the three distinct unsteady flow phenomena revealed by experiment[5] could be identified in the computational results.

## Results and Discussion

The numerical results presented here were obtained using a time-accurate, thin-layer Navier-Stokes solver[6] over an ogive-cylinder body. The code has been extensively tested and used during the last several years to solve many similar flowfields and compared successfully against other three-dimensional Navier-Stokes solvers, parabolized Navier-Stokes solvers, and experiments (cf. Refs. 6–8) for supersonic and subsonic turbulent and laminar flows.

The results were obtained for Mach number 0.2, laminar flows with Reynolds number based on freestream conditions and cylinder diameter of $2.6 \times 10^4$, and angles of attack of 40 and 60 deg. The body consisted of a 3.5-diam tangent ogive

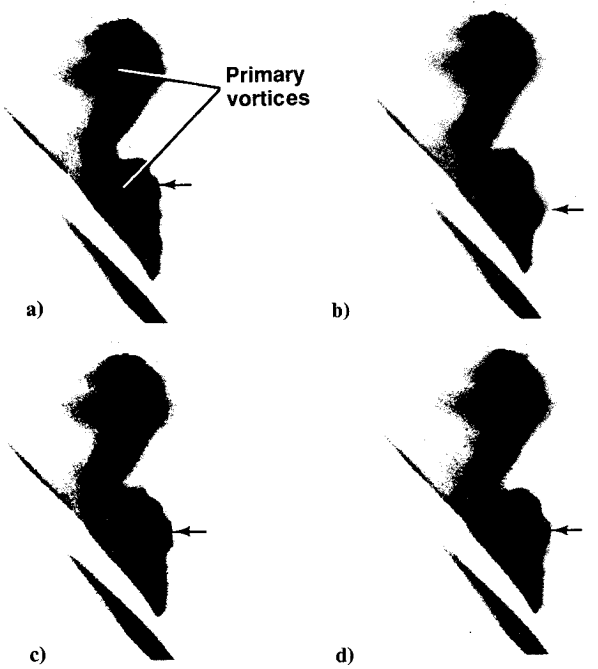


**Fig. 1 Time sequence smoke visualization of flowfield above an ogive-cylinder configuration: $x/D = 5.4$, $\alpha = 40$ deg, $Re_D = 2.6 \times 10^4$.**

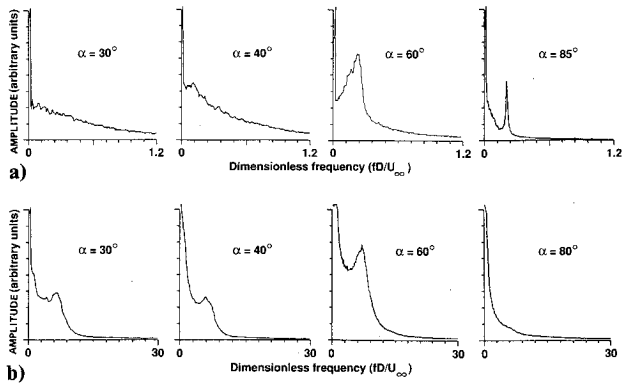


**Fig. 2 Effect of angle of attack on pressure power spectra at $x/D = 5.4$, $Re_D = 2.6 \times 10^4$: a) low-frequency range; b) high-frequency range.**

forebody with a 7.0-diam cylindrical afterbody. The grid that was used for the numerical simulation consisted of 120 equispaced circumferential planes, extending completely around the body. In each circumferential plane, the grid had 50 radial and 59 axial points. The computations were started from undisturbed freestream conditions, and the governing flow equations were advanced in time to obtain time histories of the evolution of the flows. In order to excite the stationary asymmetric mode,[4,8] a small perturbation was placed near the apex. If the perturbation was placed farther aft on the body, the flow asymmetry was reduced almost to zero.

For both angles of attack, the cores of the primary vortices fluctuate at a low frequency around a mean with time, but also small highly elongated vortices, which are generated in the shear layer near the body surface and have the same sense of rotation as the primary vortices, may move up the shear layer and merge into the primary vortices, in a way similar to the experimental findings.[5] Figures 3a–d show a sequence of successive helicity density cross-section contours of the flowfield at $\alpha = 40$ deg and $x/D = 5.4$. (Helicity density is defined as the scalar product of the local velocity and vorticity vectors.[9] It indicates both the strength and sense of rotation of the vortices.) If the shear-layer vortex, which is marked by 1, is followed, the process of its movement up the shear layer until it merges into the primary vortex becomes clear. At the same time, a new vortex is formed under it (marked by 2) and follows the same history. It was suggested[9] that helicity density can represent the geometrical properties of a vortex, and by comparing Figs. 3 and 1, one can appreciate the qualitative agreement between the experiment and computation. It was also observed from the computed surface flow patterns of these cases (Figs. 4) that several small regions of unsteadiness existed between the primary and secondary crossflow separation lines on both sides of the cylindrical portion of the body (indicated by the arrows in Figs. 4), qualitatively similar to experimental findings.[3]

The power spectra of the computed surface pressure that were recorded at the same station as in the experiment[5] ($x/D = 5.4$, Figs. 2) are given in Figs. 5. Two main frequencies can be seen. The dominant low-frequency peak ($S \approx 0.1$ for $\alpha = 40$ deg and $S \approx 0.18$ for $\alpha = 60$ deg) is associated with unsteadiness of the primary vortices (which will develop eventually to von Kármán vortex shedding as the angle of attack increases). The high-frequency peak ($S \approx 2.2$ for both cases) is associated with the passage of small vortices along the shear layer. The moderate frequencies shown in Figs. 4. ($S \approx 0.5$) could well be an indication of vortex interaction as suggested in Ref. 5. Obviously, the numerical spectra presented here do not have as wide a range of frequencies as found in the experiments (especially for the low-frequency range), probably because of the coarse grid used and numerical dissipation. However, the cluster of low-frequency peaks near $S = 0.18$ for $\alpha = 60$ deg could be the beginning of the formation of the

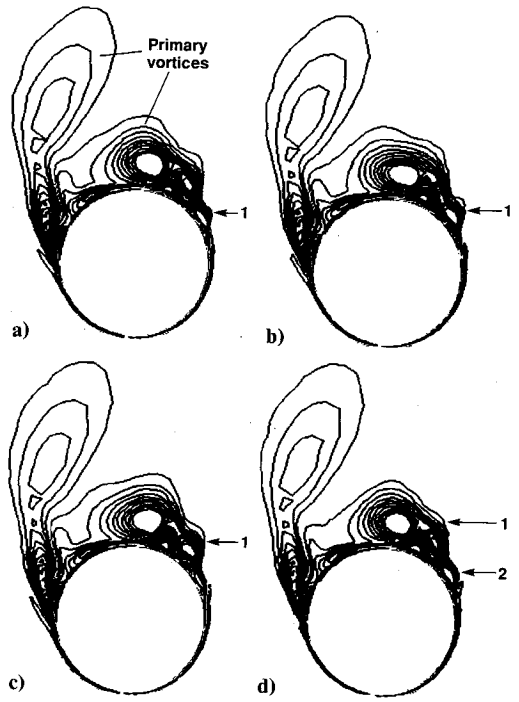


**Fig. 3 Successive helicity density contours planes: $x/D=5.4$, $\alpha=40$ deg, $M_\infty=0.2$, $Re_D=2.6\times10^4$, laminar flow.**

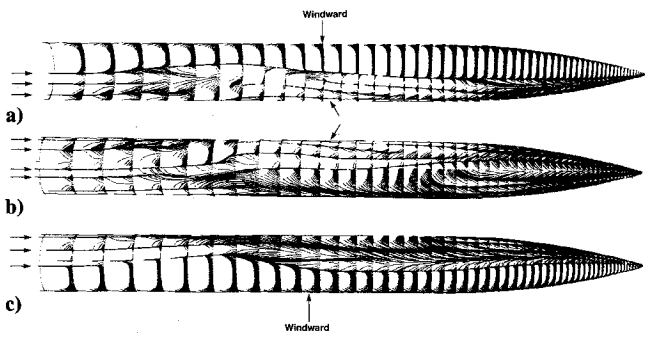


**Fig. 4 Computed surface flow pattern; $\alpha=40$ deg, $M_\infty=0.2$, $Re_D=2.6\times10^4$, laminar flow: a) left-side view; b) top view; c) right-side view.**

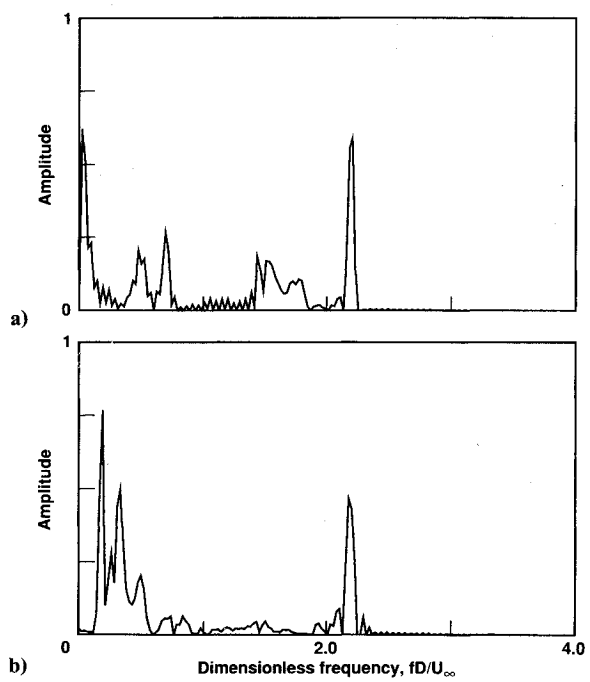


**Fig. 5 Computed surface pressure power spectra at $x/D=5.4$, $M_\infty=0.2$, $Re_D=2\times10^4$: a) $\alpha=40$ deg; b) $\alpha=60$ deg.**

larger cluster of frequencies that was found experimentally near the same $S$ value.

When the space-fixed perturbation was removed, the flowfield relaxed back to its original symmetric shape,[8] and, therefore, it was suggested[10] that the symmetric flow at these angles of attack is convectively unstable. This suggestion was supported by recent experimental findings.[11] Nevertheless, the shear-layer vortices were not affected by symmetry changes of the flowfield and continued to move at about the same frequency (although with some changes in location). Similarly, placing a splitter plate[12] along the leeward plane of symmetry, which forced the flow to become symmetric (and suppressed the low-frequency shedding), did not affect the high-frequency shear-layer unsteadiness.

When the Reynolds number was increased to $2\times10^5$, both for $\alpha=40$ and 60 deg, similar behavior was found. The main difference was that the low-frequency peaks were obtained at higher $S$ values than those obtained for the lower Reynolds number case.

## Conclusions

Numerical results obtained with a three-dimensional, thin-layer Navier-Stokes solver qualitatively follow the experimental findings and show that at least two main frequencies exist on an ogive cylinder at angles of attack of 40 and 60 deg: a low frequency associated with fluctuations of the primary vortices that leads to vortex shedding and a high frequency associated with fluctuations of the shear layer. The shear-layer fluctuations, as evident in the computed surface flow patterns, are concentrated in several small areas above the leeward side of the cylindrical portion of the body. The existence of midrange peaks in the computed power spectra suggests that the experimentally observed[5] vortex interaction fluctuations may also be present in the computed flowfield.

## References

[1]Kourta, A., Boisson, H. C., Chassaing, P., and Minh, H. H., "Nonlinear Interaction and the Transition to Turbulence in the Wake of a Circular Cylinder," *Journal of Fluid Mechanics,* Vol. 181, 1987, pp. 141–161.

[2]Wei, T., and Smith C. R., "Secondary Vortices in the Wake of Circular Cylinders," *Journal of Fluid Mechanics,* Vol. 169, 1986, pp. 513–533.

[3]Poll, D. I. A., "Some Observations of the Transition Process on the Windward Face of a Long Yawed Cylinder," *Journal of Fluid Mechanics,* Vol. 150, 1985, pp. 329–356.

[4]Degani, D., and Schiff, L. B., "Numerical Simulation of Asymmetric Vortex Flows Occurring on Bodies of Revolution at Large Incidence," AIAA Paper 87-2628, Aug. 1987.

[5]Degani, D., and Zilliac, G. G., "Experimental Study of Nonsteady Asymmetric Flow Around an Ogive-Cylinder at Incidence," *AIAA Journal,* Vol. 28, No. 4, 1990, pp. 642–649.

[6]Steger, J. L., Ying, S. X., and Schiff, L. B., "A Partially Flux-Split Algorithm for Numerical Simulation of Unsteady Viscous Flows," *Proceedings of a Workshop on Computational Fluid Dynamics,* Univ. of California, Davis, CA, 1986.

[7]Schiff, L. B., Degani, D., and Cummings, R. M., "Numerical Simulation of Separated and Vortical Flows on Bodies at Large Angles of Attack," *Fourth Symposium — Numerical and Physical Aspects of Aerodynamics Flows,* Long Beach, Jan. 1989.

[8]Degani, D., and Schiff, L. B., "Numerical Simulation of the Effect of Spatial Distrubances on Vortex Asymmetry," AIAA Paper 89-0340, Jan. 1989.

[9]Levy, Y., Degani, D., and Seginer, A., "Graphical Visualization of Vortical Flows by Means of Helicity," *AIAA Journal,* Vol. 28, No. 8, 1990, pp. 1347–1352.

[10]Degani, D., "Numerical Investigation of the Origin of Vortex Asymmetry," AIAA Paper 90-0593, Jan. 1990.

[11]Degani, D., and Tobak, M., "Numerical, Experimental, and Theoretical Study of Convective Instability of Flows Over Pointed Bodies at Incidence," AIAA Paper 91-0291, Jan. 1991.

[12]Degani, D., "Effect of Splitter Plate on Unsteady Flows Around a Body of Revolution at Incidence," *Physics of Fluids A,* Vol. 3, No. 9, 1991, pp. 2122–2130.